Reconstructing Mars Atmospheric Reentry using an Unscented Kalman Filter

Abinay J. Brown
Georgia Institute of Technology, Atlanta, Georgia, 30332

This research project demonstrates the application of the Unscented Kalman Filter (UKF) in reconstructing the Mars' hypersonic reentry trajectory of a spacecraft and estimating Mars' atmospheric density using simulated accelerometer and altimetry data. The UKF accurately modeled the nonlinear dynamics involved in atmospheric reentry, showing only minor deviations from the simulated nominal trajectory. Notably, the UKF predicted the landing site with a slight deviation of approximately 0.674 km from the nominal site, underscoring its precision. The filter effectively captured the exponential variation of atmospheric density with altitude with a max standard deviation of $0.000456(kg/m^3)$. Tunning the UKF filter parameters further, specifically the process noise covariance matrix, as well as increasing the sensor sampling frequency to 200Hz, reduced the estimation errors. Overall, the UKF's proved to be successful for the purposes of the profiling atmospheric density and hypersonic reentry trajectories for the purposes of future Mars' missions.

I. Nomenclature

V	=	Reentry Velocity
χ	=	Heading Angle
γ	=	Flight Path Angle
σ	=	Bank Angle
h	=	Altitude
Rm	=	Mars Radius
rho	=	Air Density
C_d	=	Drag Coefficient
m	=	Mass
L/D	=	Lift to Drag Ratio
H	=	Scale Height
L	=	Lift
D	=	Drag
g	=	acceleration due to gravity
μ	=	Mars gravitational Parameter
r	=	Distance from Mars Center
Rm	=	Mars Radius
Xe	=	World Frame Position X
Ye	=	World Frame Position Y
Ze	=	World Frame Position Z

II. Introduction

Mars exploration has been a significant focus of NASA's space missions over the past decades. These missions have been instrumental in gathering data about the Martian atmosphere, surface, and potential for past life, and therefore expanding our knowledge about the Red Planet and improving technologies for future space exploration. One of the important aspects of these missions is landing a probe on the surface which involves Hypersonic atmospheric reentry process, where spacecraft must withstand high thermal and mechanical stresses as they descend through the atmosphere. Accurate modeling and simulation of this reentry are paramount not only for the success of the mission but

also for the safety of the craft and its payload.

Historically, atmospheric reentry missions have employed various data collection techniques to study the entry, descent, and landing (EDL) phases. These missions, such as Mars Pathfinder, Mars Exploration Rovers (Spirit and Opportunity), and the Mars Science Laboratory (Curiosity rover), have utilized accelerometers and altimeters among other instruments to collect valuable data during the reentry phase [1]. This data helps in reconstructing the trajectory and understanding the atmospheric interaction with the spacecraft. For instance, during the Mars Science Laboratory mission, the use of a guided entry system demonstrated an advanced capability in precision landing, which heavily relied on accurate atmospheric modeling derived from sensor data [2].

The Mars missions have contributed to the development of aerospace technologies and enhance our predictive capabilities related to atmospheric conditions. These advancements are crucial for future missions, including potential human exploration of Mars and exploration of other planetary bodies as well.

In this research, we investigate the implementation of an Unscented Kalman Filter (UKF) to recreate the hypersonic reentry trajectory using simulated accelerometer and altimetry data and to also estimate the density-altitude profile of the Martian atmosphere in the process. The accelerometer data should provide the net forces acting on the reentry vehicle, and the altimetry data should provide the reference above ground necessary for reconstructing the trajectory. Assuming that the forces acting on the vehicle are just gravity, lift, and drag, with gravity being known, we could possibly determine the density given the lift and drag equations since the net acceleration is known. The UKF is known for its efficacy in handling nonlinear systems well, and is therefore used in this application to avoid complexities and modeling errors due to linearization and approximations.

III. Methodology

A. Atmospheric Reentry Equations of Motion

The Reentry equations of motion are given below in equations 1 to 4 [3]. In this project, an uncontrolled atmospheric reentry is assumed to simplify the problem in order that only the filtering and reconstruction aspect is focused on. The Equations of motion are modelled and simulated in the Trajectory Reference Frame and constant bank angle descent have been assumed.

$$\dot{V} = \frac{-D}{m} - g\sin(\gamma) \tag{1}$$

$$\dot{\chi} = \frac{L\sin(\sigma)}{mVcos(\gamma)} \tag{2}$$

$$\dot{\gamma} = \frac{L\cos(\sigma)}{mV} + \cos(\gamma)(\frac{V}{r} - \frac{g}{V}) \tag{3}$$

$$\dot{h} = V\sin(\gamma) \tag{4}$$

The other parameters that are a function of the state variables that plug into the dynamics above such as air density, drag, lift, and gravitational acceleration are calculated using the following equations below. The air density is taken as an exponential model [4], with a quadratic drag force. Additionally, it is assumed that the Lift to Drag Ratio of the Vehicle remains constant throughout the entire phase of reentry to simplify the implementation.

$$\rho = \rho_0 e^{-h/H} \tag{5}$$

$$D = \frac{1}{2} rho * V^2 * C_d * A \tag{6}$$

$$L = (L/D) * D \tag{7}$$

$$g = \frac{\mu}{r^2} \tag{8}$$

$$r = R_m + h \tag{9}$$

The Reentry Parameters/Constants, as well as the Reentry Vehicle Parameters used in the simulation can be summarized in the table 1 provided below. The vehicle parameters were chosen to be nearly the the same properties of the Mars 2020 reentry vehicle [5].

Table 1 Mars Constants and Vehicle Parameters

Parameter	Value
μ	$4.2828 * 10^{13} \frac{m^3}{s^2}$
R_m	$3376.2km$
ρ_0	$0.02 \frac{kg}{m^3}$
σ	2.5^o
H	$11.1km$
M	$3520kg$
A	$63.62m^2$
C_d	1.7
L/ D	0.3

B. Unscented Kalman Filter

The Unscented Kalman Filter (UKF) utilizes the unscented transform to estimate the state of a nonlinear system[6]. Initially, at each integration step of the system, 2N sigma points are generated around the current state estimate to effectively capture its mean and covariance characteristics Eq(10). Each of these sigma points are propagated through the nonlinear process model to predict the next state Eq(11). The covariance of these predicted states is then updated by incorporating process noise to reflect the uncertainty of the prediction Eq(12).

$$\chi_{k|k-1} = \begin{bmatrix} \hat{x}_{k-1} \\ \hat{x}_{k-1} + \sqrt{(L+\lambda)P_{k-1}} \\ \hat{x}_{k-1} - \sqrt{(L+\lambda)P_{k-1}} \end{bmatrix} \tag{10}$$

$$\hat{x}_{k|k-1} = \sum_{i=0}^{2L} W_i^{(m)} f(\chi_{i,k-1}) \tag{11}$$

$$P_{k|k-1} = \sum_{i=0}^{2L} W_i^{(c)} [f(\chi_{i,k-1}) - \hat{x}_{k|k-1}][f(\chi_{i,k-1}) - \hat{x}_{k|k-1}]^T + Q_k \tag{12}$$

The sigma points are also used to predict the measurement output by passing them through the measurement model, here it is the world frame velocities and altitude, resulting in a predicted measurement Eq(13). The covariance of the predicted measurement is then calculated to assess the prediction's uncertainty, including the measurement noise Eq(14).

$$\hat{z}_{k|k-1} = \sum_{i=0}^{2L} W_i^{(m)} h(\chi_{i,k-1}) \tag{13}$$

$$P_{k|k-1}^{zz} = \sum_{i=0}^{2L} W_i^{(c)} [h(\chi_{i,k-1}) - \hat{z}_{k|k-1}][h(\chi_{i,k-1}) - \hat{z}_{k|k-1}]^T + R_k \tag{14}$$

A cross-covariance matrix between the state and the measurements is computed Eq(15). This matrix is crucial for updating the state estimate as it quantifies the extent to which changes in the state estimate affect the predicted measurement. Using this matrix, the Kalman gain is calculated Eq(16), which determines how much the prediction should be corrected based on the new measurement.

Finally, the actual state update is performed using the new measurement to adjust the predicted state, and therefore refining the state estimate Eq(17). The corresponding covariance of the state is also updated to decrease the uncertainty following the measurement update Eq(18). These steps are then repeated recursively at each time step to refine the state estimates as newer sensor data are processed.

$$P^{xz}_{k|k-1} = \sum_{i=0}^{2L} W_i^{(c)} [f(\chi_{i,k-1}) - \hat{x}_{k|k-1}][h(\chi_{i,k-1}) - \hat{z}_{k|k-1}]^T \tag{15}$$

$$K_k = P^{xz}_{k|k-1} (P^{zz}_{k|k-1})^{-1} \tag{16}$$

$$\hat{x}_{k|k} = \hat{x}_{k|k-1} + K_k (z_k - \hat{z}_{k|k-1}) \tag{17}$$

$$P_{k|k} = P_{k|k-1} - K_k P^{zz}_{k|k-1} K_k^T \tag{18}$$

C. Simulating Accelerometer and Altimetry Data

For the purposes of simulating the sensor data the for the given initial conditions, a nominal reentry trajectory is generated. The nominal trajectory is then used to convert to world frame velocity using the following transformation from trajectory frame to world frame given below.

$$\dot{X}_e = V \cos(\gamma) \cos(\chi) \tag{19}$$

$$\dot{Y}_e = V \cos(\gamma) \sin(\chi) \tag{20}$$

$$\dot{Z}_e = -V \sin(\gamma) \tag{21}$$

The World frame velocities are then interpolated using splines and then differentiated using finite differencing method to determine the nominal trajectory xyz accelerations in the world frame.

Ideally, the sensor frame acceleration are used by converting it to the vehicle frame and then to the world frame using dynamic transformations through vehicle attitude estimates, but for the sake of simplicity of the equations of motion and scope of the project, simulated accelerometer measurements are directly taken in the World frame by adding random noise to generated nominal world frame acceleration.

Similarly, random noise is added to the nominal altitude data as well to simulate altimetry sensor data for the Filtering runs. The noise added to the Accelerometer and Altimetry data can be summarized in the table 2 below.

Table 2 Sensor Noise Parameters

Parameter	Value
σ_{ax}	$0.1 m/s^2$
σ_{ay}	$0.1 m/s^2$
σ_{az}	$0.1 m/s^2$
σ_h	$1m$

D. Reconstructing Reentry Trajectory and Estimating Density

In the UKF implementation, an auxiliary state variable, density parameter, is appended to the state vector given below along with the initial conditions.

$$X = [V, \chi, \gamma, h, \rho]^T \tag{22}$$

$$X_0 = [5.5km/s, 0deg, -12deg, 135km, 1.0449 * 10^{-7} kg/m^3]^T \tag{23}$$

$$P_0 = diag([1, 0.1, 0.1, 1, 10^{-10}]) \tag{24}$$

When propagating the sigma points using the EOM in 1-4, the original density equation 5 is replaced by this density parameter from the state vector in order that the UKF can estimate the density as a function of altitude along with other states that best models the trajectory from the noisy measurements. The EOM for density is left as 0.

For the measurements, the noisy world frame simulated sensor accelerations are numerically integrated using trapezoidal method to get the noisy world frame velocities that are to be used as measurements along with the noisy altitude data directly in the UKF. On integrating the noisy accelerometer, the errors propagate and and the standard deviations in the velocity measurements grow as a function of time at each time step. The measurement vector and the measurement noise covariance used for reconstruction is given below.

$$z = [\dot{X}e, \dot{Y}e, \dot{Z}e, h]^T \tag{25}$$

$$R = \begin{bmatrix} \sum_{i=1}^{n} \sigma_{ax,i}^2 \Delta t^2 & 0 & 0 & 0 \\ 0 & \sum_{i=1}^{n} \sigma_{ay,i}^2 \Delta t^2 & 0 & 0 \\ 0 & 0 & \sum_{i=1}^{n} \sigma_{az,i}^2 \Delta t^2 & 0 \\ 0 & 0 & 0 & \sigma_h^2 \end{bmatrix} \tag{26}$$

The predicted measurement of the system at each time step can be found using the state vector by Eq 19-21 and is used to determine the correction required for the state. Finally the Process noise covariance used for the filter is given below. They were selected based on performance and converges of the filter by iterative and intuitively trying different values.

$$Q = diag([0.005, 0.0001, 0.0001, 0.0001, 10^{-7}]) \tag{27}$$

On following the recursive steps of UKF, a filtered trajectory fit and estimated atmospheric density can be found.

IV. Results

A. Reentry trajectory

The Simulated Nominal Trajectory of the Hypersonic Reentry along with recreated UKF estimated is shown below in Figure 1. There is a slight deviation in the estimated landing site.

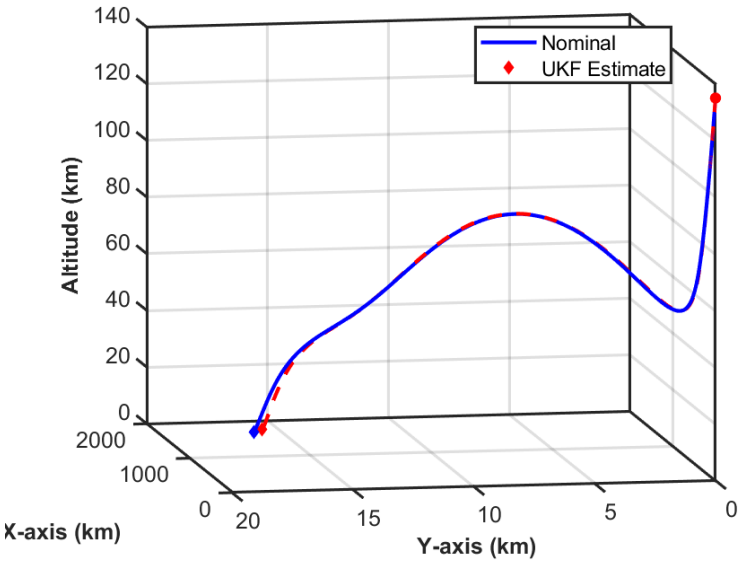

Fig. 1 Reconstructed 3D Trajectory

B. Estimated Reentry States

The UKF State estimates is plotted alongside the simulated nominal states to visualize the performance of the UKF in recreating the trajectory individually. Figures 2-5 depict the reentry velocity, heading angle, flight path angle, and height profiles of the recreated trajectory, respectively. On this scale, this state estimates are almost identical with only a slight deviation in the heading angle estimate.

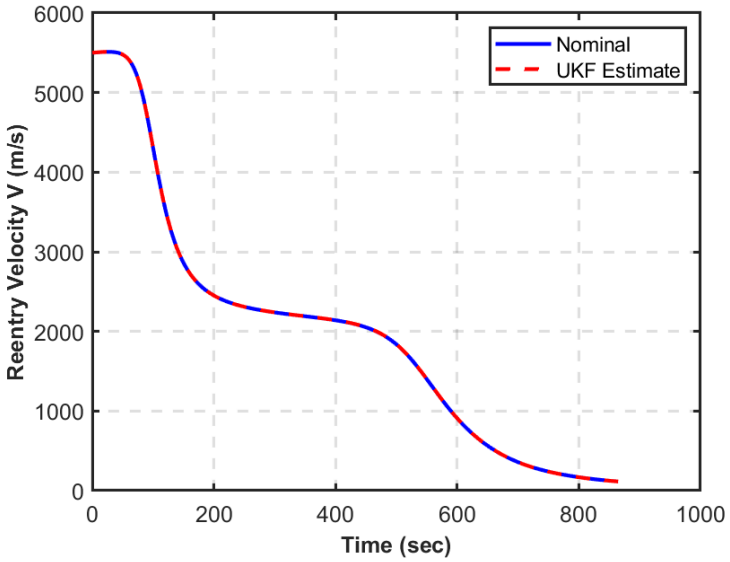

Fig. 2 Reentry Velocity Profile and the UKF Estimate

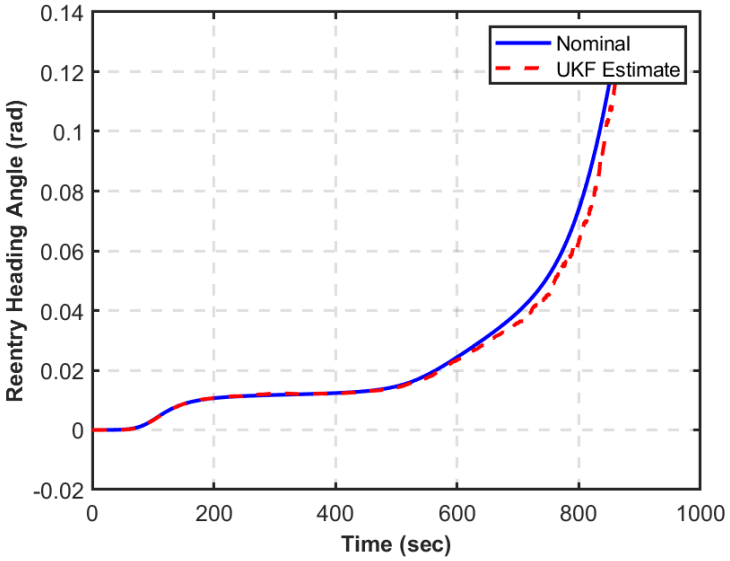

Fig. 3 Heading Angle Profile and the UKF Estimate

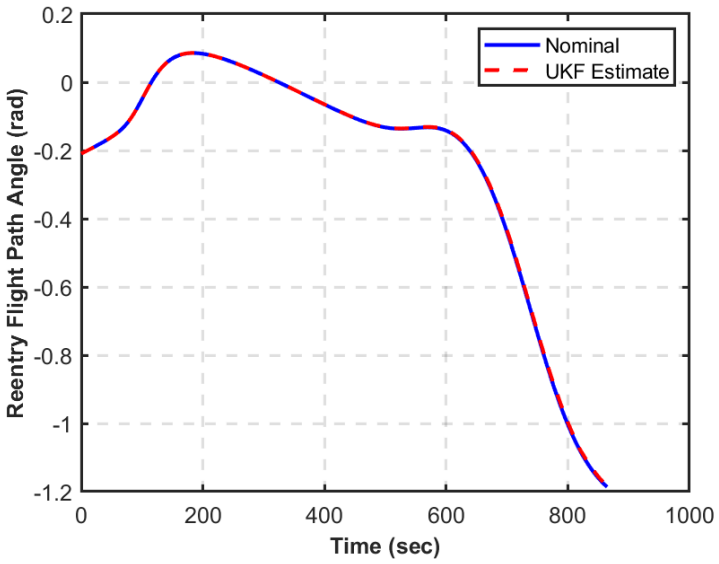

Fig. 4 Flight Path Angle Profile and the UKF Estimate

C. Estimated Atmospheric Density Profile

The Atmospheric Density was almost accurately estimated by the UKF. It was able to accurately capture the exponential varying density as a function of altitude simply by recreating the trajectory as seen in figure 6.

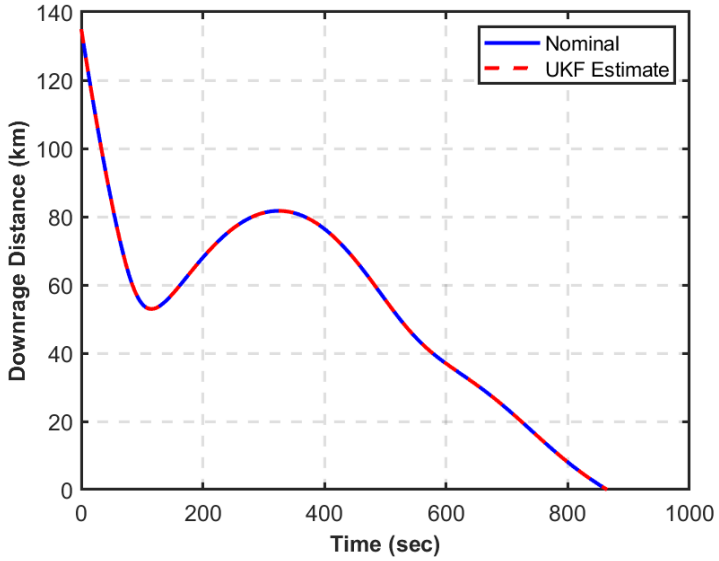

Fig. 5 Altitude Profile and the UKF Estimate

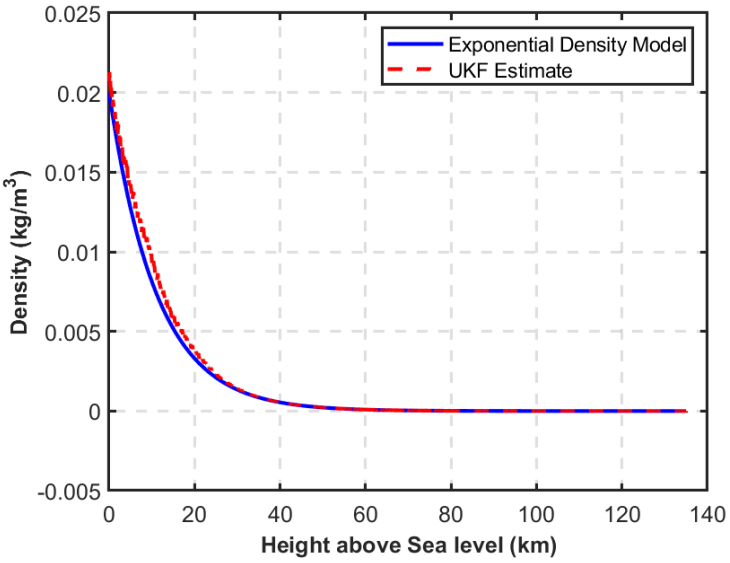

Fig. 6 Mars Exponential Density and the UKF Density Estimate

Figure 7 below shows the variance in the Density estimate as a function of time, and it is inherent that the variance in the estimate increases in the order of 10^{-6} as the vehicle is closes the the ground at about 40km. Mars' atmosphere is very thin and therefore at higher altitudes the atmospheric densities are almost neglible which is why the variance is lower at higher altitude.

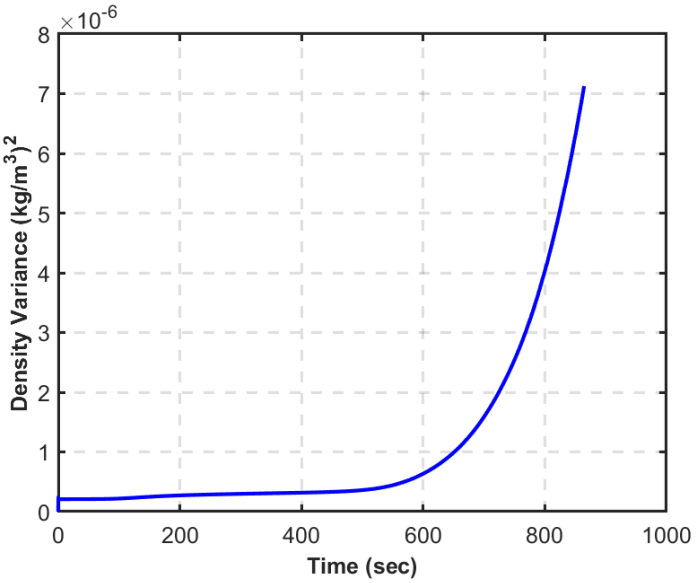

Fig. 7 Variance of the Density estimates

D. Error Analysis

The steady state covariances of the estimated state variables are summarized in the table 3 below. This was found by taking mean values of after the point where the Variances were nearly constant.

Table 3 Estimated Variances

Steady State Covariance	Value
σ_V^2	$0.1217(m/s)^2$
σ_χ^2	$4.56 * 10^{-4}(rad)^2$
σ_γ^2	$2.75 * 10^{-4}(rad)^2$
σ_h^2	$0.0285m^2$

Table 4 below gives the Nominal landing location and the estimated landing location as comparison for the performance of the UKF in predicting the landing site.

Table 4 Sensor Noise Parameters

$X_{Nom}(km)$	$Y_{Nom}(km)$	$X_{UKF}(km)$	$Y_{UKF}(km)$
1695.42	16.091	1695.99	15.74

V. Discussion

The application of the Unscented Kalman Filter (UKF) in this study provided significant insights into its robustness and precision in reconstructing the hypersonic reentry trajectory of a spacecraft entering Mars' atmosphere. It allowed for better modeling nonlinearities without approximation or linearization of the dynamic model or the observation model reducing the overall complexity of the implementation which is important for such applications where the dynamics could get more complex making it computationally intensive to linearize at each time step.

The reconstructed trajectory, as illustrated in Figure 1 showed minimal deviations from the simulated nominal trajectory, it is important to note that the minor deviations and errors can also be attributed to the discrete trapezoidal integration of the UKF estimated velocities to recreate the trajectory. Additionally, the reconstructed state variables in figures 2-5 show that the states were accurately estimated with a slight deviation in the estimated heading angle as well as atmospheric density, this can be improved by tuning the UKF parameters, such as the process noise covariance matrix, which could reduce the estimation error.

Initially setting the process noise covariance matrix to zero led the UKF to diverge completely from the nominal trajectory. On introducing some process noise weights, especially for the density parameter, the UKF was better able to converge and accurately model the states and the density variations as well. Tunning of the Q matrix further will results in finer results.

The atmospheric density profile (Figure 6) demonstrated the UKF's capability to effectively capture the exponential increase in density with altitude. The filter showed an increase in variance of the estimated density closer to the ground in the order of $10^{-6}(kg/m^3)^2$ as seen in figure 7. This is because the Martian atmosphere is very thin and almost negligible at higher altitudes than near the ground.

The initial error covariance matrix was taken as a random guess and had assumed values, during the UKF run, the error covariance immediately reached steady state values, as seen in Table 3, state error covariances settled to a much lower value than assumed initially. The associated error covariances of velocity (0.1217 m^2/s^2) and altitude (0.0285 m^2) suggest that while the UKF performs well under the conditions tested, the integration of noisy accelerometer data—which directly influences velocity and subsequently altitude calculations as well. For this simulation a sensor frequency of 50Hz were chosen since higher frequency observation required computation time of over 30 minutes, increase the sampling frequency can reduces the direct integration errors. Additionally, the euclidean distance error in the estimated and nominal landing site is about 0.674km.

To model the uncertainty in the predicted landing site, multiple runs with generated noisy sensor data can be used to predict landing locations; known as the Monte Carlo Analysis[7]. This can used to generate landing ellipse that shows the region of high landing probability. Since this requires running multiple variations of noisy sensor data to determine the predicted landing sites, with each run taking over 10 minutes, more computing power and parallelized resources are required to generate such an analysis.

This project served as an initially assessment to implement and test how the UKF can be used for application of reconstructing atmospheric reentry as well as characterizing a planet's atmospheric density. For more realistic applications, a better dynamic model that includes other dynamically changing state variables such as latitude, longitudes rates, as well as variable bank angles, with higher order density models can significantly increase the fidelity and accuracy of the simulation. Additionally, using real accelerometer data in conjunction to attitude estimates that transform body frame acceleration to inertial frame would make it a more realistic process of using sensor data for filtering.

VI. Conclusion

This study successfully utilized the Unscented Kalman Filter (UKF) to reconstruct the trajectory of a Mars' atmospheric reentry, showing its effectiveness in accurately modeling complex dynamics just from simulated accelerometer and altimetry data. The UKF closely matched the expected trajectory with minor deviations due to discrete integration, confirming its precision. The UKF was able to model the exponentially varying atmospheric density accurately as well. Tunning the UKF parameters improved its performance, particularly in estimating atmospheric density. Challenges in initial settings, such as the process noise covariance matrix, were overcome by fine-tuning the parameters, enhancing the filter's stability and accuracy. It is also determined that increase sampling frequency improved the performance. Further improvements can be made by refining the model by including more dynamic variables that influence the trajectory and by including a higher order density model. Additionally, Monte-Carlo Analysis can be used analyze the landing site prediction and its errors.

Appendix

The code included with this project inlcudes the "PlotStateVector.m", "PlotCovariances.m", and "PlotTrajectory.m" that will directly plot the generated results that are saved in the Nominal.mat as well as the UKF.mat files.

To generate the UKF results directly requires running the 'Kalman2main.m' which takes roughly 10mins to perform the calculations and output the results to the .mat files. During the runs, the current iteration and total iterations will be printed in the command window to show the run progress. The 'Kalman2main.m' function directly uses the 'UKF.m' function that implements the modified dynamics for the UKF propagation.

To generate the nominal results, running the "Nominal.m", will output the results into the "Nominal.mat" file and plot the trajectory as well. To generate noisy simulated sensor data, running the "SensorData.m" file will generate and store the sensor data into the SensorData.mat file.

Acknowledgments

Abinay J. Brown thanks Professor Brian C. Gunter from the Daniel Guggenheim School of Aerospace Engineering at Georgia Tech for providing resources to learn about Random Process and Kalman Filtering and for inspiring this project.

References

[1] Karlgaard, C. D., Kutty, P., Schoenenberger, M., Shidner, J., and Munk, M., "Mars Entry Atmospheric Data System Trajectory Reconstruction Algorithms and Flight Results," *American Institute of Aeronautics and Astronautics*, 2013. Paper presented at the AIAA Guidance, Navigation, and Control Conference.

[2] Way, D. W., Powell, R. W., Chen, A., Steltzner, A. D., Martin, A. M. S., Burkhart, P. D., and Mendeck, G. F., "Mars Science Laboratory: Entry, Descent, and Landing System Performance," *IEEE Aerospace Conference*, Big Sky, MT, 2006, pp. 3–10. Paper Number: 1467.

[3] Zhao, J., and Li, S., "Mars atmospheric entry trajectory optimization with maximum parachute deployment altitude using adaptive mesh refinement," *Acta Astronautica*, Vol. 160, 2019, pp. 401–413. https://doi.org/10.1016/j.actaastro.2019.03.027, URL https://www.sciencedirect.com/science/article/pii/S0094576518310609.

[4] NASA Glenn Research Center, "Mars Atmosphere Model - Metric Units," https://www.grc.nasa.gov/www/k-12/airplane/atmosmrm.html, 2021. Accessed: Insert date here.

[5] Wikipedia contributors, "Mars 2020," https://en.wikipedia.org/wiki/Mars_2020, 2023. Accessed: 28th April 2024.

[6] Julier, S. J., and Uhlmann, J. K., "A New Extension of the Kalman Filter to Nonlinear Systems," *Proc. of AeroSense: The 11th Int. Symposium on Aerospace/Defense Sensing, Simulation and Controls*, Vol. 3, 1997, pp. 182–193.

[7] Hash, D. B., and Hassan, H. A., "Monte Carlo simulation of entry in the Martian atmosphere," *Journal of Thermophysics and Heat Transfer*, Vol. 7, No. 2, 1993, pp. 228–232. https://doi.org/10.2514/3.411, URL https://doi.org/10.2514/3.411.